A probabilistic model of resistance jumps in memristive devices

Valeriy A. Slipko*,† and Yuriy V. Pershin*,‡

†Institute of Physics, Opole University, Opole 45-052, Poland ‡Department of Physics and Astronomy, University of South Carolina, Columbia, SC 29208 USA

E-mail: vslipko@uni.opole.pl; pershin@physics.sc.edu

Abstract

Resistance switching memory cells such as electrochemical metallization cells and valence change mechanism cells have the potential to revolutionize information processing and storage. However, the creation of deterministic resistance switching devices is a challenging problem that is still open. At present, the modeling of resistance switching cells is dominantly based on deterministic models that fail to capture the cycle-to-cycle variability intrinsic to these devices. Herewith we introduce a state probability distribution function and associated integrodifferential equation to describe the switching process consisting of a set of stochastic jumps. Numerical and analytical solutions of the equation have been found in two model cases. This work expands the toolbox of models available for resistance switching cells and related devices, and enables a rigorous description of intrinsic physical behavior not available in other models.

Keywords

Resistance switching, memristive devices, stochastic switching

Resistance switching memory cells (also known as memristive devices¹) are emerging components with memory that find applica-

tions in neuromorphic, ^{2–4} logic, ^{5,6} and reservoir computing circuits, ⁷ to name a few. Over the last decade, significant progress has been achieved in the above mentioned and related areas, and includes the demonstration of high-density crossbar arrays, ⁸ diffusive memristors, ⁹ etc. Moreover, the utilization of natural materials and unconventional fabrication techniques ¹⁰ may lead to memory cells that have a lower carbon footprint compared to silicon-based electronics.

Traditionally, memristive devices have been described in terms of deterministic models. The dynamical system approach introduced by Chua and Kang¹ provides the mainstream theoretical framework (examples of memristive models can be found in Refs. 11–13). However, being relatively simple, deterministic models neglect the stochastic behavior in particular common to electrochemical metallization (ECM) cells¹⁴ and valence change mechanism (VCM) cells¹⁵ – the most typical memristive devices. As an example, Fig. 1 shows the current-voltage curve for $Cu/AlO_x/W$ non-volatile memory structure. ¹⁶

In the present paper, we develop a continuous probabilistic model to describe the evolution of stochastic memristive devices. The main assumption in the model is that the resistance switching occurs via random markovian jumps in the continuous space of internal state variable(s). Previously, we have pioneered the use of a master equation as a tool for exam-

ining the response of stochastic memristive devices with discrete states, ¹⁷ implemented this approach in SPICE, ¹⁸ and developed a theory of circuits combining discrete stochastic memristive devices with reactive components. ¹⁹ Recently, the master equation was used in the analysis of memristive Ising circuits, ²⁰ which are the electronic circuit realization of the Ising model. The present paper extends the discrete master equation approach ^{17,18,21} to a more realistic case of continuous internal states.

To take into account the stochasticity, we introduce the state probability distribution function p(x,t), where $x \in [a,b]$ is the internal state variable responsible for memory, and p(x,t)dx is the probability to find the state in the interval from x to x + dx at the time moment t. The state probability distribution function is normalized to 1:

$$\int_{a}^{b} p(x,t) dx = 1. \tag{1}$$

The first equation in the model is a statistically averaged Ohm's law

$$\langle I \rangle = \left\langle \frac{V}{R(x,V)} \right\rangle \equiv \overline{R}^{-1}(V) \cdot V, \quad (2)$$

where $\langle I \rangle$ is the mean current, V is the voltage across the device, R(x,V) is the state- and voltage-depend resistance, and $\bar{R}(V) = \left(\int_a^b R^{-1}(x,V)p(x,t)\mathrm{d}x\right)^{-1}$ is the harmonic mean resistance. We emphasize that $\bar{R}(V) \neq \langle R(x,V) \rangle$.

The evolution of p(x,t) is represented by an integro-differential equation

$$\frac{\partial p(x,t)}{\partial t} = \int_{a}^{b} \gamma(x', x, V(x')) p(x', t) dx'$$
$$-p(x,t) \int_{a}^{b} \gamma(x, x', V(x)) dx', \qquad (3)$$

which is the second equation in the model. Here, $\gamma(y, z, V(y))$ is the voltage-dependent transition rate density from internal state y to

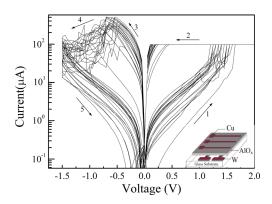


Figure 1: Experimental current-voltage curves of $\text{Cu/AlO}_x/\text{W}$ nonvolatile memory structure (for details, see Ref. 16). Reprinted from Ref. 16.

z, and V(y) is the voltage across the device in state y. The first term in the right hand side of (3) describes the transitions to x from all other states, while the second one – the reverse transitions.

The extension of Eqs. (2), (3) to several internal state variables is discussed in the Supporting Information (SI).

To illustrate the above model, we consider two special cases of Eqs. (2) and (3). In both cases, we will use the resistance $R \in [R_{on}, R_{off}]$ as the internal state variable, $x \equiv R$, and the resistance probability distribution function, r(R, t), as the state probability distribution function. Here, R_{on} and R_{off} denote the ON and OFF state resistance, respectively.

In the first model, we assume a uniform continuous distribution of jumps in the direction defined by the applied voltage. The transition rate density in Eq. (3) is selected as

$$\gamma(R', R, V) = \begin{cases} \alpha_{10} e^{\frac{|V|}{V_{10}}} &, V > 0, R' < R \\ \alpha_{01} e^{\frac{|V|}{V_{01}}} &, V < 0, R' > R \\ 0 &, \text{ otherwise} \end{cases}$$
(4)

where α_{10} , V_{01} , and α_{01} , V_{01} are the coefficients defining the transition rates in the direction from ON to OFF (10) and OFF to ON (01) resistance state, respectively, and the exponential dependence on voltage is selected based on experimental observations. ^{22–24} Below, we use the notation $\gamma_{10} = \alpha_{10} \exp(|V|/V_{10})$ corresponding to the top line in the rhs of Eq. (4).

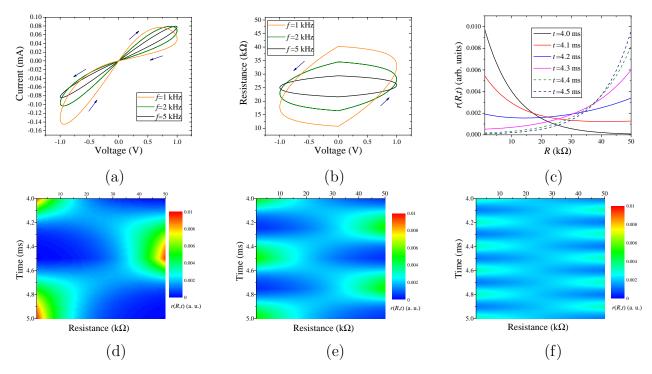


Figure 2: First model simulations. Response to a sinusoidal voltage $V = V_0 \sin{(2\pi ft)}$: (a) mean current-voltage curves, (b) $\langle R \rangle(t)$ versus voltage, (c) resistance distribution function at selected times (f = 1 kHz), and (d)-(f) color plots of r(R, t) at f = 1, 2, 5 kHz, respectively. This figure was obtained using the following parameter values: $R_{on} = 1 \text{ k}\Omega$, $R_{off} = 50 \text{ k}\Omega$, $\alpha_{10} = \alpha_{01} = 0.1 \text{ (s} \cdot \Omega)^{-1}$, and $V_{10} = V_{01} = V_0 = 1 \text{ V}$.

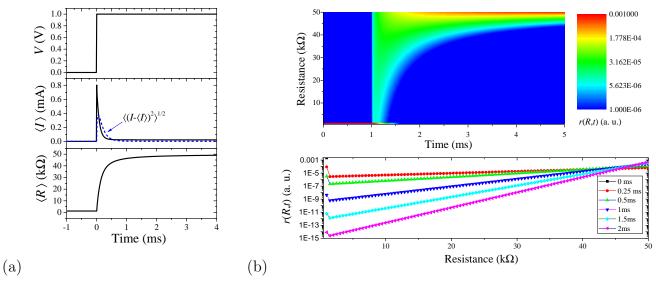


Figure 3: First model simulations. Response to a step-like voltage: (a) Voltage, mean current and mean resistance as functions of time, (b) color plot (log scale) of r(R,t) (top), and r(R,t) at selected times (bottom). This figure was obtained using the same parameter values as in Fig. 2 and $r(R,0) = \delta(R - R_{on})$.

Fig. 2 shows results of numerical simulations for the above model in the case of sinusoidal driving. We note that the frequency behavior of current-voltage curves in Fig. 2(a) is typical to memristive devices. Within each period, the maximum of the resistance distribution function r(R,t) drifts from R_{ON} to R_{OFF} and back. Note that Fig. 2(c) shows the evolution in the first half-period of periodic driving. Panels (d)-(f) in Fig. 2 demonstrate that the resistance distribution function becomes less localized at higher frequencies. Overall, all these results are not unexpected.

Next, we simulate the response to step voltage (Fig. 3). According to Fig. 3(a), the step voltage switches the resistance from R_{on} to R_{off} in a relatively short time interval. A notable feature is the exponential decay in the resistance probability distribution function as seen in the bottom panel in Fig. 3(b).

The analytical solution of Eq. (3) with γ given by Eq. (4) and V = const can be found using the method of Laplace transform. One can show (see SI) that the general solution for V > 0 can be written as

$$r(R,t) = \gamma_{10} t e^{-\gamma_{10}(R_{off} - R)t} \int_{R_{on}}^{R} r(R', 0) dR' + r(R, 0) e^{-\gamma_{10}(R_{off} - R)t}, \quad (5)$$

where r(R,0) is the initial resistance probability distribution function.

The simple form of the general solution (5) allows the detailed analysis of the evolution for any initial resistance probability distribution function r(R,0). Consider, for instance, $r(R,0) = \delta(R - R_{on})$ (the detailed analysis of this case is given in SI). One can easily see that the probability distribution function decreases purely exponentially at the left edge of the distribution (at $R = R_{on}$) with the highest possible rate $\gamma_{10}(R_{off} - R_{on})$:

$$r(R_{on}, t) = r(R_{on}, 0)e^{-\gamma_{10}(R_{off} - R_{on})t}.$$
 (6)

At the right edge of the resistance interval, the resistance probability distribution function growths linearly from t = 0:

$$r(R_{off}, t) = r(R_{off}, 0) + \gamma_{10}t.$$
 (7)

This result corresponds to the fact that at the positive voltage, the resistance can only increase (or stay constant), see Eq. (4). This leads to the accumulation of the probability density at $R = R_{off}$. It also follows directly from Eq. (5) that inside of the interval $[R_{on}, R_{off}]$, r(R,t) increases first and then decreases. The decrease is exponenntial with R-dependent rate $\gamma_{10}(R_{off} - R)$. Moreover, the linear growth of probability (7) at R_{off} implies that the characteristic width of the distribution peak decreases as $(\gamma_{10}t)^{-1}$ asymptotically in time.

Eq. (5) allows finding various quantities on average such as the mean resistance

$$\langle R \rangle(t) = R_{off} - \frac{1 - e^{-\gamma_{10}(R_{off} - R_{on})t}}{\gamma_{10}t}$$
 (8)

and its variance (see SI).

In the second model we use R-dependent transition rates to describe the situation when the shorter jumps are more frequent than longer. The transition rate density is selected as

$$\gamma(R, R', V) = \begin{cases} \alpha_{10} e^{\frac{|V|}{V_{10}} - \frac{|R - R'|}{R_0}}, V > 0, \ R < R' \\ \alpha_{01} e^{\frac{|V|}{V_{01}} - \frac{|R - R'|}{R_0}}, V < 0, \ R > R' \\ 0, \text{ otherwise} \end{cases}$$
(9)

where R_0 defines the average size of the jump. In fact, the first model can be considered as the limiting case of the second model in the limit of $R_0 \to \infty$.

Fig. 4 shows the response of the second model to step voltage. We highlight a couple of interesting features of this result. First, unlike Fig. 3(a), in Fig. 4(a) there is a significant interval of the linear growth of resistance (from 0 ms to 1.5 ms). Second, the resistance probability distribution function is more localized: in the bottom panel of Fig. 4(b) there is a clear peak that shifts from left to right as the resistance switches from R_{on} to R_{off} .

Compared to the first model, the analytic analysis of the second one is more involved. Its

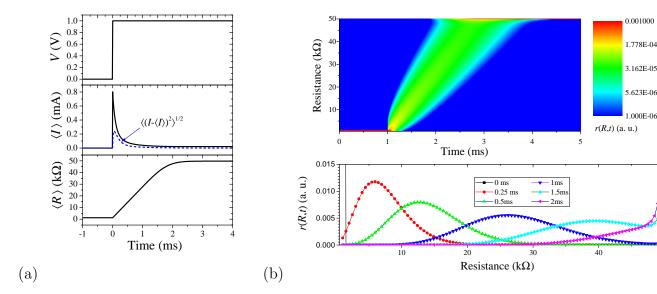


Figure 4: Second model simulations. Response to a step-like voltage: (a) Voltage, mean current and mean resistance as functions of time; (b) color plot (log scale) of r(R,t) (top), and r(R,t) at selected times (bottom). This figure was obtained using the following parameter values: $R_{on} = 1 \text{ k}\Omega$, $R_{off} = 50 \text{ k}\Omega$, $\alpha_{10} = \alpha_{01} = 10 \text{ (s} \cdot \Omega)^{-1}$, $V_{10} = V_{01} = 1 \text{ V}$, $R_0 = 1 \text{ k}\Omega$, and $r(R,0) = \delta(R - R_{on})$.

general solution is complex (we give it in SI, see Eq. (S.17) supplemented by Eq. (S.18)). This exact analytical solution allows the efficient numerical calculation of the resistance probability distribution function r(R,t) at any moment of time for the whole range of parameters, in particular for small values of R_0 . Moreover, it allows the derivation of simple asymptotic formulas for interesting limiting cases.

In particular, the solution for $r(R, 0) = \delta(R - R_{on})$ (given by Eq. (S.22) in SI) allows to calculate directly the mean resistance and its variance at short times,

$$\langle R \rangle = R_{on} + R_0^2 \gamma_{10} t, \tag{10}$$

and

$$\langle (R - \langle R \rangle)^2 \rangle = 2R_0^3 \gamma_{10} t. \tag{11}$$

In fact, Eqs. (10), (11) are exact in the limit of $R_{off} \to \infty$ in Eq. (S.22). Note that Eq. (10) explains the linear increase of $\langle R \rangle$ in Fig. 4(a).

Additionally, if $\gamma_{10}t(R-R_{on}) = \gamma_{10}R_0t\xi \gg 1$, the solution (S.22) can be simplified to

$$r(R,t) = \frac{(\gamma_{10}R_0t)^{1/4}}{2\sqrt{\pi}\xi^{3/4}R_0}e^{-(\sqrt{\xi}-\sqrt{\gamma_{10}R_0t})^2}, \quad (12)$$

where, for shortness, we have introduced ξ

$$(R-R_{on})/R_0$$
.

From Eq. (12) we see that far from both boundaries, R_{on} and R_{off} , the resistance probability distribution function r(R,t) tends asymptotically to the bell-shaped distribution (Eq. (12)) at $t \gg 1/(\gamma_{10}R_0\xi)$. tion of the maximum, $\xi_{max} = \xi_{max}(t)$, can be easily calculated from Eq. (12). At long times, $\gamma_{10}R_0t \gg 1$, we find that $\xi_{max}(t) =$ $\gamma_{10}R_0t - 3/2 + O(1/t)$. It means that in this regime the distribution maximum, ξ_{max} , propagates at constant velocity $\gamma_{10}R_0^2$ in the R-space. The magnitude of the distribution maximum $r(\xi_{max}(t),t) = 1/(2R_0\sqrt{\pi\gamma_{10}R_0t})(1+O(1/t))$ decreases as the inverse square root of time. This also means that the characteristic width of the probability distribution increases as the square root of time (to satisfy the normalization condition). Another way to see it is to expand up to quadratic terms with respect to $(\xi - \xi_{max})$ the logarithm of Eq. (12). This way we get the following approximated expression for the probability distribution function (12), which is valid in the vicinity of the maximum point $\xi_{max}(t)$ when $\gamma_{10}R_0t \gg 1$:

$$r(R,t) = \frac{1}{2R_0\sqrt{\pi\gamma_{10}R_0t}}e^{-\frac{(\xi-\gamma_{10}R_0t+3/2)^2}{4\gamma_{10}R_0t}}.$$
 (13)

Eq. (13) is the Gaussian distribution with the maximum at $\xi_{max} \approx \gamma_{10} R_0 t - 3/2$ and standard deviation $\sqrt{2\gamma_{10}R_0t}$.

Thus we see that the evolution of the initial delta function distribution $r(R, t) = \delta(R - R_{on})$ involves three stages (when $|R_{off} - R_{on}| \gg$ R_0). At the first stage, $0 < t \lesssim (\gamma_{10}R_0)^{-1}$, the "running wave", which is described by the second term in Eq. (S.22), is formed near R_{on} . At the second stage, $(\gamma_{10}R_0)^{-1} \lesssim t \lesssim$ $(R_{off} - R_{on})/(\gamma_{10}R_0^2)$, as the first term in Eq. (S.22) becomes exponentially small, the second term, which can be approximated by Eq. (12), describes the propagation of the "wave" at constant velocity $\gamma_{10}R_0^2$ and its broadening as $2R_0\sqrt{\pi\gamma_{10}R_0t}$ in R-space. At the beginning of the last third stage of evolution, $t \gtrsim (R_{off} - R_{on})/(\gamma_{10}R_0^2)$, the "wave" reaches R_{off} . At this moment of time, the probability distribution has a characteristic width of $2\sqrt{\pi R_0(R_{off}-R_{on})}$, which is much larger than R_0 (by a factor of $\sim 2\sqrt{\pi(R_{off}-R_{on})/R_0} \gg$ 1), and, at the same time, much smaller than $(R_{off} - R_{on})$. Therefore, the probability distribution stays localized the whole evolution time. Eventually, the magnitude of the probability distribution at R_{off} starts to grow linearly in time, $r(R_{off},t) \sim \gamma_{10}t$, as it follows from the asymptotic behavior of Laplace transform $\tilde{r}(R_{off},p) \sim \gamma_{10}/p^2$ when $p \to 0$. At the same time, the probability distribution approaches the delta function $\delta(R - R_{off})$.

In conclusion, we have developed a fundamentally different probabilistic model of memristive devices that takes into account the cycleto-cycle variability in their response. Our model differs conceptually from the conventional memristive models in its statistical approach to the description of resistance switching phenomenon. Overall, this work provides a new tool for the analysis of stochastic memristive devices and their circuits.

Acknowledgement The authors are thankful to each other for productive collaboration resulted in this paper.

Supporting Information Available

Details of the solutions; extension of the model to several internal state variables.

References

- (1) Chua, L. O.; Kang, S. M. Memristive Devices and Systems. *Proc. IEEE* **1976**, *64*, 209–223.
- (2) Li, Y.; Wang, Z.; Midya, R.; Xia, Q.; Yang, J. J. Review of memristor devices in neuromorphic computing: materials sciences and device challenges. *Journal of Physics D: Applied Physics* **2018**, *51*, 503002.
- (3) Xia, Q.; Yang, J. J. Memristive crossbar arrays for brain-inspired computing. *Nature materials* **2019**, *18*, 309–323.
- (4) Christensen, D. V. et al. 2022 roadmap on neuromorphic computing and engineering. Neuromorphic Computing and Engineering 2022, 2, 022501.
- (5) Vourkas, I.; Sirakoulis, G. C. Emerging memristor-based logic circuit design approaches: A review. *IEEE circuits and systems magazine* **2016**, *16*, 15–30.
- (6) Sebastian, A.; Le Gallo, M.; Khaddam-Aljameh, R.; Eleftheriou, E. Memory devices and applications for in-memory computing. *Nature nanotechnology* **2020**, *15*, 529–544.
- (7) Kulkarni, M. S.; Teuscher, C. Memristorbased reservoir computing. 2012 IEEE/ACM international symposium on nanoscale architectures (NANOARCH). 2012; pp 226–232.
- (8) Pi, S.; Li, C.; Jiang, H.; Xia, W.; Xin, H.; Yang, J. J.; Xia, Q. Memristor crossbar arrays with 6-nm half-pitch and 2-nm critical dimension. *Nature nanotechnology* **2019**, *14*, 35–39.

- (9) Wang, Z.; Joshi, S.; Savel'ev, S. E.; Jiang, H.; Midya, R.; Lin, P.; Hu, M.; Ge, N.; Strachan, J. P.; Li, Z., et al. Memristors with diffusive dynamics as synaptic emulators for neuromorphic computing. *Nature materials* **2017**, *16*, 101–108.
- (10) Kim, J.; Dowling, V. J.; Datta, T.; Pershin, Y. V. Whisky-born memristor. *physica status solidi* (a) **2022**, n/a, 2200643.
- (11) Kvatinsky, S.; Friedman, E. G.; Kolodny, A.; Weiser, U. C. TEAM: Threshold adaptive memristor model. *IEEE transactions on circuits and systems I: regular papers* **2012**, *60*, 211–221.
- (12) Strachan, J. P.; Torrezan, A. C.; Miao, F.; Pickett, M. D.; Yang, J. J.; Yi, W.; Medeiros-Ribeiro, G.; Williams, R. S. State dynamics and modeling of tantalum oxide memristors. *IEEE Transactions on Electron Devices* 2013, 60, 2194–2202.
- (13) Pershin, Y. V.; Di Ventra, M. Memory effects in complex materials and nanoscale systems. *Advances in Physics* **2011**, *60*, 145–227.
- (14) Valov, I.; Waser, R.; Jameson, J. R.; Kozicki, M. N. Electrochemical metallization memories—fundamentals, applications, prospects. *Nanotechnology* 2011, 22, 254003.
- (15) Yang, J. J.; Inoue, I. H.; Mikolajick, T.; Hwang, C. S. Metal oxide memories based on thermochemical and valence change mechanisms. MRS bulletin 2012, 37, 131– 137.
- (16) Sleiman, A.; Sayers, P. W.; Mabrook, M. F. Mechanism of resistive switching in Cu/AlO_x/W nonvolatile memory structures. *Journal of Applied Physics* 2013, 113, 164506.
- (17) Dowling, V. J.; Slipko, V. A.; Pershin, Y. V. Probabilistic memristive networks: Application of a master equation to networks of binary ReRAM cells.

- Chaos, Solitons & Fractals **2021**, 142, 110385.
- (18) Dowling, V.; Slipko, V.; Pershin, Y. Modeling Networks of Probabilistic Memristors in SPICE. *Radioengineering* **2021**, 30, 157–163.
- (19) Slipko, V. A.; Pershin, Y. V. Theory of heterogeneous circuits with stochastic memristive devices. *IEEE Transactions on Circuits and Systems II: Express Briefs* **2021**, *69*, 214–218.
- (20) Dowling, V. J.; Pershin, Y. V. Memristive Ising circuits. *Phys. Rev. E* **2022**, *106*, 054156.
- (21) Ntinas, V.; Rubio, A.; Sirakoulis, G. C. Probabilistic resistive switching device modeling based on Markov jump processes. *IEEE Access* **2021**, *9*, 983–988.
- (22) Jo, S. H.; Kim, K.-H.; Lu, W. Programmable resistance switching in nanoscale two-terminal devices. *Nano letters* **2009**, *9*, 496–500.
- (23) Gaba, S.; Sheridan, P.; Zhou, J.; Choi, S.; Lu, W. Stochastic memristive devices for computing and neuromorphic applications. *Nanoscale* **2013**, *5*, 5872–5878.
- (24) Naous, R.; Siemon, A.; Schulten, M.; Alahmadi, H.; Kindsmüller, A.; Lübben, M.; Heittmann, A.; Waser, R.; Salama, K. N.; Menzel, S. Theory and experimental verification of configurable computing with stochastic memristors. Scientific reports 2021, 11, 1–11.

Supporting Information

A probabilistic model of resistance jumps in memristive devices

Valeriy A. Slipko¹ and Yuriy V. Pershin²

E-mails: vslipko@uni.opole.pl; pershin@physics.sc.edu

Uniform distribution of jumps

Laplace transform solution

To solve the integro-differential equation (3) with γ given by Eq. (4) at constant V > 0, we introduce the Laplace transform in the time domain as $\tilde{r}(R,p) = \int_0^\infty r(R,t) \exp(-pt) dt$. Applying the Laplace transformation to Eq. (3) one obtains

$$[p + \gamma_{10}(R_{off} - R)] \tilde{r}(R, p) = \gamma_{10} \int_{R_{on}}^{R} \tilde{r}(R', p) dR' + r(R, 0),$$
 (S.1)

where $r(R,0) \equiv r(R,t=0)$ is the initial resistance probability distribution function.

By differentiating Eq. (S.1) with respect to R, we arrive at a first-order non-homogeneous linear differential equation with the following general solution

$$\tilde{r}(R,p) = \frac{r(R,0)}{[p + \gamma_{10}(R_{off} - R)]} + \frac{C(p) + \gamma_{10} \int_{R_{on}}^{R} r(R',0) dR'}{[p + \gamma_{10}(R_{off} - R)]^2},$$
(S.2)

where C(p) is an arbitrary function. Consider now Eq. (S.1) at $R = R_{on}$. Its solution is $\tilde{r}(R_{on}, p) = r(R_{on}, 0)/[p + \gamma_{10}(R_{off} - R_{on})]$. Comparing this expression with Eq. (S.2) at $R = R_{on}$, we find that C(p) = 0. The inverse Laplace transform leads to the following general solution of Eq. (3):

$$r(R,t) = \gamma_{10} t e^{-\gamma_{10}(R_{off} - R)t} \int_{R_{on}}^{R} r(R',0) dR' + r(R,0) e^{-\gamma_{10}(R_{off} - R)t} .$$
 (S.3)

Solution analysis

To illustrate the solution (S.3), let us consider the evolution of the resistance initially localized at $R = R_{on}$. Such situation is described by the initial resistance probability distribution function $r(R,0) = \delta(R - R_{on})$, where δ is the Dirac delta function. From Eq. (S.3) it follows that at any moment of time the probability distribution is the sum of two terms:

$$r(R,t) = \delta(R - R_{on})e^{-\gamma_{10}(R_{off} - R_{on})t} + \gamma_{10}te^{-\gamma_{10}(R_{off} - R)t}.$$
 (S.4)

¹Institute of Physics, Opole University, Opole 45-052, Poland

²Department of Physics and Astronomy, University of South Carolina, Columbia, SC 29208, USA

The first term corresponds to the initial distribution function, whose magnitude decreases exponentially in time with the highest possible rate $\gamma_{10}(R_{off} - R_{on})$ in the system (due to transitions into the continuum of states $R_{on} < R \le R_{off}$). The second term grows at the initial period of time until $t(R) = (\gamma_{10}(R_{off} - R))^{-1}$. Later, at t > t(R), the second term asymptotically decreases to zero everywhere except of $R = R_{off}$, where the probability distribution function accumulates with time.

These properties of the distribution function are reflected in the behavior of the mean resistance as a function of time that can be calculated by using Eq. (S.4):

$$\langle R \rangle (t) = \int_{R_{on}}^{R_{off}} r(R, t) R dR = R_{off} - \frac{1 - e^{-\gamma_{10}(R_{off} - R_{on})t}}{\gamma_{10}t}.$$
 (S.5)

The mean resistance changes linearly with time at short times $\gamma_{10}(R_{off}-R_{on})t\ll 1$ starting at the value R_{on}

$$\langle R \rangle(t) = R_{on} + \frac{\gamma_{10}t}{2} (R_{off} - R_{on})^2, \ t \to 0,$$
 (S.6)

and reaching asymptotically the value R_{off} at long times $\gamma_{10}(R_{off}-R_{on})t\gg 1$ in accordance with the law

$$\langle R \rangle(t) = R_{off} - \frac{1}{\gamma_{10}t}, \ t \to \infty.$$
 (S.7)

Similarly we can calculate the variance of resistance

$$\langle (R - \langle R \rangle)^2 \rangle = \frac{1 - 2\gamma_{10}t(R_{off} - R_{on})e^{-\gamma_{10}(R_{off} - R_{on})t} - e^{-2\gamma_{10}(R_{off} - R_{on})t}}{(\gamma_{10}t)^2},$$
(S.8)

with the following asymptotic behavior at short and long times

$$\langle (R - \langle R \rangle)^2 \rangle = \frac{\gamma_{10}t}{3} (R_{off} - R_{on})^3, \text{ when } \gamma_{10} (R_{off} - R_{on})t \ll 1, \tag{S.9}$$

and

$$\langle (R - \langle R \rangle)^2 \rangle = \frac{1}{(\gamma_{10}t)^2}, \text{ when } \gamma_{10}(R_{off} - R_{on})t \gg 1.$$
 (S.10)

Thus we see that being initially localized at R_{on} , the resistance probability distribution expands into R-space due to transitions into all states with $R > R_{on}$. The distribution goes through the transient period of time in the region (R_{on}, R_{off}) , and it gradually accumulates in the vicinity of the boundary point R_{off} , asymptotically in time.

It is interesting to note that precise analytical solution (S.3) can be used to express the mean resistance at any moment of time t through the resistance probability distribution function at t = 0:

$$\langle R \rangle(t) = R_{off} - \frac{1}{\gamma_{10}t} + \frac{1}{\gamma_{10}t} \int_{R_{op}}^{R_{off}} dR \ r(R,0)e^{-\gamma_{10}(R_{off}-R)t}.$$
 (S.11)

By expending the exponential function $e^{\gamma_{10}Rt}$ in Eq. (S.11), we can demonstrate how the mean resistance $\langle R \rangle(t)$ explicitly depends on all the moments $\langle R \rangle(0)$, $\langle R^2 \rangle(0)$, ... at the initial moment

of time t = 0:

$$\langle R \rangle(t) = R_{off} + \frac{e^{-\gamma_{10}R_{off}t} - 1}{\gamma_{10}t} + e^{-\gamma_{10}R_{off}t} \sum_{n=1}^{+\infty} \frac{(\gamma_{10}t)^{n-1}}{n!} \langle R^n \rangle(0).$$
 (S.12)

Because all the moments can be independently specified, the mean resistance depends in principle on the infinite number of parameters (the initial moments). Consequently, in general, there is no differential equation of finite order, which could describe the evolution of the mean resistance for an arbitrary initial condition. But if we limit the class of the initial conditions considering, for example, only deterministic initial conditions, $r(R, 0) = \delta(R - R_i)$ with some initial resistance R_i , then the corresponding dynamic differential equations for the mean resistance can be found.

Non-uniform distribution of jumps

Laplace transform solution

In this section we consider the dynamics of the second model in the presence of a positive constant voltage. The substitution of the transition rate $\gamma(R', R, V_M)$ from Eq. (9) into Eq. (3) leads to

$$\frac{\partial g(R,t)}{\partial t} = \gamma_{10} \int_{R_{on}}^{R} g(R',t) dR' - \Gamma(R)g(R,t), \tag{S.13}$$

where $g(R,t) = r(R,t)e^{R/R_0}$ is a new (non-normalized) resistance probability distribution function. In the above equation, we have also introduced the rate

$$\Gamma(R) = \gamma_{10} R_0 \left(1 - \exp\left\{ (R - R_{off}) / R_0 \right\} \right).$$
 (S.14)

In the Laplace domain, the general solution of Eq. (S.13) with arbitrary initial condition r(R, 0) is given by

$$\tilde{r}(R,p) = \frac{r(R,0)}{p+\Gamma(R)} + \int_{R_{on}}^{R} \Phi(p,R,R_1) r(R_1,0) dR_1,$$
(S.15)

where $\Phi(p, R, R_1)$ is the regular single-valued on the whole complex plane, except for the branch cut $[-\Gamma(R_1), -\Gamma(R)]$, branch of the analytic function of complex variable p:

$$\Phi(p, R, R_1) = \frac{\gamma_{10}}{(p + \Gamma(R))^2} \exp\left\{\frac{p}{p + R_0 \gamma_{10}} \left[\ln \frac{p + \Gamma(R)}{p + \Gamma(R_1)} - \frac{R - R_1}{R_0} \right] \right\}, \tag{S.16}$$

defined by the condition that the logarithm function is real, $\Im\left(\ln\frac{p+\Gamma(R)}{p+\Gamma(R_1)}\right)=0$, when p>0. It can be easily verified that such a branch has a removable singularity at $p=-R_0\gamma_{10}$. Moreover, the function $\Phi(p,R,R_1)$ is analytic at infinity with the following asymptotic behavior: $\Phi(p,R,R_1)=\gamma_{10}\exp\left((R_1-R)/R_0\right)/p^2$ as $p\to\infty$.

By using these properties of the Laplace transform, we can present the inverse Laplace transform as the integral in the complex p-plane along any curve C, which encircles the branch cut in the positive (counterclockwise) direction. For further calculations, it is convenient to make the linear fractional transformation $\zeta = R_0 \gamma_{10}/(p + \Gamma(R))$. As a result of this transformation, the general

solution of Eq. (S.13) can be presented as

$$r(R,t) = r(R,0)e^{-\Gamma(R)t} + e^{-\Gamma(R)t} \int_{R_{on}}^{R} \frac{dR_1}{R_0} r(R_1,0) \exp\left\{-\frac{R-R_1}{R_0}\right\} I(t,R,R_1),$$
 (S.17)

where we have introduced the contour integral over the unit circle in the counter-clockwise direction

$$I(t, R, R_1) = \frac{1}{2\pi i} \oint_{|\zeta|=1} \frac{\mathrm{d}\zeta}{1 + [\delta - \delta_1]\zeta} \exp\left\{\frac{\gamma_{10}R_0t}{\zeta} + \frac{\zeta\left(\ln\left[1 + (\delta - \delta_1)\zeta\right] + \frac{R - R_1}{R_0}\right)}{1 + \zeta\delta}\right\},\tag{S.18}$$

where $\delta = \delta(R) = \exp((R - R_{off})/R_0)$, and $\delta_1 = \delta(R_1)$.

While analyzing the integrand in Eq. (S.18), it is useful to note that $0 < \delta_1 < \delta \le 1$ since $R_{on} \le R_1 < R \le R_{off}$.

Solution analysis

First of all, let us check that solution given by Eqs. (S.17) and (S.18) coincides with solution (5) in the case when $(R_{off} - R_{on}) \ll R_0$. For this purpose we have to replace δ and δ_1 with 1 in Eq. (S.18). As a result, we find that

$$I(t, R, R_1) = \frac{1}{2\pi i} \oint_{|\zeta|=1} d\zeta \exp\left\{\frac{\gamma_{10} R_0 t}{\zeta}\right\} = \gamma_{10} R_0 t, \ R_0 \to \infty.$$

This result along with the observation that $\Gamma(R) \to \gamma_{10}(R_{off} - R)$, when $R_0 \to \infty$, shows that general solution (S.17), (S.18) transforms to solution (5) in the limiting case $(R_{off} - R_{on}) \ll R_0$ as it should be.

In the opposite limiting case $(R_{off} - R_{on}) \gg R_0$, the general solution (S.17), (S.18) also can be simplified in the domain far from the right end R_{off} , where $|R_{off} - R| \gg R_0$. In this case both δ and δ_1 are exponentially small, so we can replace them with zeroes in Eq. (S.18). Thus we obtain the following approximate expression

$$I(t, R, R_1) = \frac{1}{2\pi i} \oint_{|\zeta|=1} d\zeta \exp\left\{\frac{\gamma_{10}R_0t}{\zeta} + \zeta \frac{(R-R_1)}{R_0}\right\} = R_0\gamma_{10}t \sum_{k=0}^{+\infty} \frac{[\gamma_{10}t(R-R_1)]^k}{k!(k+1)!}, \quad (S.19)$$

when $R_0 \to 0$. By using the power series expansion of the modified Bessel function of the first kind, $\sum_{k=0}^{+\infty} \frac{x^k}{k!(k+1)!} = I_1(2\sqrt{x})/\sqrt{x}$, we get

$$I(t, R, R_1) = R_0 \gamma_{10} t \frac{I_1(2\sqrt{\gamma_{10}t(R - R_1)})}{\sqrt{\gamma_{10}t(R - R_1)}}, \text{ when } |R_{off} - R| \gg R_0.$$
 (S.20)

Eq. (S.20) along with Eq. (S.17) allow us to write the general solution of Eq. (3) in the following compact form

$$r(R,t) = r(R,0)e^{-\gamma_{10}R_0t} + \gamma_{10}te^{-\gamma_{10}R_0t} \int_{R_{on}}^{R} dR_1 r(R_1,0)e^{-\frac{R-R_1}{R_0}} \frac{I_1(2\sqrt{\gamma_{10}t(R-R_1)})}{\sqrt{\gamma_{10}t(R-R_1)}}, \quad (S.21)$$

for the domain where $|R_{off} - R| \gg R_0$.

To illustrate the evolution of the distribution function determined by solution (S.21), we consider the initial condition in the form of the delta function $r(R,0) = \delta(R - R_{on})$. The delta function initial distribution corresponds to the initial state of memristor when resistivity R equals R_{on} with probability 1. In this case, we immediately get from Eq. (S.21)

$$r(R,t) = e^{-\gamma_{10}R_0t}\delta(R - R_{on}) + \gamma_{10}te^{-\gamma_{10}R_0t - \frac{R - R_{on}}{R_0}} \frac{I_1(2\sqrt{\gamma_{10}t(R - R_{on})})}{\sqrt{\gamma_{10}t(R - R_{on})}},$$
 (S.22)

for the domain where $|R_{off} - R| \gg R_0$.

Several internal state variables

Here we briefly discuss the extension of Eqs. (2)-(3) model to devices described by N > 1 internal state variables $\{x_1, ..., x_N\} \equiv \mathbf{x}$. Here, the bold font is used to denote a vector.

In the case of several internal state variables, the state probability distribution function is $p(\mathbf{x}, t)$, and its normalization is given by

$$\int_{a_1}^{b_1} \dots \int_{a_N}^{b_N} p(\mathbf{x}, t) dx_1 \dots dx_N = 1.$$
 (S.23)

The limits of integration in the above integrals depend on the physical nature of state variables and are generally different for different variables.

The first equation in the model is exactly the same as Eq. (2). The only difference is that the mean current is evaluated with the help of N integrals

$$\langle I \rangle (t) = \int_{a_1}^{b_1} \dots \int_{a_N}^{b_N} \frac{V(t)}{R(\mathbf{x}, t)} p(\mathbf{x}, t) dx_1 \dots dx_N.$$
 (S.24)

The evolution of $p(\mathbf{x},t)$ is represented by

$$\frac{\partial p(\mathbf{x},t)}{\partial t} = \int_{a_1}^{b_2} \dots \int_{a_N}^{b_N} \left[\gamma(\mathbf{x}', \mathbf{x}, V(\mathbf{x}')) p(\mathbf{x}', t) - p(\mathbf{x}, t) \gamma(\mathbf{x}, \mathbf{x}', V(\mathbf{x})) \right] dx'_1 \dots dx'_N, \tag{S.25}$$

where $\gamma(\mathbf{y}, \mathbf{z}, V(\mathbf{y}))$ is the voltage-dependent transition rate density from \mathbf{y} to \mathbf{z} , and $V(\mathbf{y})$ is the voltage across the device in state \mathbf{y} .

In the situations, when the probability of the simultaneous change of two or more state variables in a single jump is infinitesimal, the transition rate may be represented by the sum of terms like $\gamma(y_1, z_1, V(\mathbf{y}))\delta(y_2 - z_2)...\delta(y_N - z_N)$, etc.

Graphical TOC Entry

